Sorting linearly polarized photons with a single scatterer

Francisco J. Rodríguez-Fortuño, Daniel Puerto, Amadeu Griol, Laurent Bellieres, Javier Martí, and Alejandro Martínez*

Nanophotonics Technology Center, Universitat Politècnica de València, Camí de Vera, 46022 Valencia, Spain
**Corresponding author: amartinez@ntc.upv.es*

Received January 9, 2014; revised January 24, 2014; accepted January 24, 2014;
posted January 24, 2014 (Doc. ID 204505); published March 5, 2014

Intuitively, light impinging on a spatially mirror-symmetric object will be scattered equally into mirror-symmetric directions. This intuition can fail at the nanoscale if the polarization of the incoming light is properly tailored, as long as mirror symmetry is broken in the axes perpendicular to both the incident wave vector and the remaining mirror-symmetric direction. The unidirectional excitation of plasmonic modes using circularly polarized light has been recently demonstrated. Here, we generalize this concept and show that linearly polarized photons impinging on a single spatially symmetric scatterer created in a silicon waveguide are guided into a certain direction of the waveguide depending exclusively on their polarization angle and the structure asymmetry. Our work broadens the scope of polarization-induced directionality beyond plasmonics, with applications in polarization (de)multiplexing, unidirectional coupling, directional switching, radiation polarization control, and polarization-encoded quantum information processing in photonic integrated circuits.

OCIS codes: (130.5440) Polarization-selective devices; (130.3120) Integrated optics devices; (130.2790) Guided waves.
http://dx.doi.org/10.1364/OL.39.001394

Polarization is a fundamental property of electromagnetic radiation that drastically increases the richness of the interaction between light and matter, enabling countless polarimetry applications and information transfer and processing based on polarization states [1,2].

It is known that shaping the polarization and amplitude of incoming pulses of light can be used to switch between propagation paths or localized spots [3–7]. Recently, a series of works have shown that the interaction of monochromatic circularly polarized light with structures having one mirror-symmetry plane can result in asymmetric excitation of surface plasmons (surface electromagnetic waves in metals) toward mirror-symmetric directions, enabling the sorting of light into different directions according to its spin [8–13]. This requires the structures to have a broken symmetry in the direction orthogonal to both the mirror-symmetric direction and the incident wave vector. This novel and somewhat unexpected property is given different interpretations, such as near field interference [8], and ultimately relies on the incoming polarization breaking the existing mirror symmetry of the structures. This powerful concept has been demonstrated for plasmonic waves, but it is so fundamental that it can be extended to any class of waveguide. In previous works, the use of circularly polarized light together with the use of surface plasmons, which inherently show high attenuation and require either the measurement of leakage radiation or near field scanning, make the experimental realization difficult and limit the practical applicability. In this work, we overcome both obstacles, first by demonstrating the concept of polarization-sorting beyond plasmonics, employing a dielectric scatterer and waveguide, thus removing optical losses, simplifying light collection, and opening the field to a broader range of scientists in nano-optics. Second, we remove the need for circular polarization and the associated lambda-quarter wave plates by designing a structure that works with linear polarization (although the method is general and valid for any polarization).

We achieve the sorting of linearly polarized photons impinging normally on a single scatterer built into a standard silicon waveguide, so that incoming photons can be directed toward each waveguide direction depending on their polarization. The technique is nonresonant although there is a relationship between the wavelength and the polarization angle required to direct photons toward opposite directions. Our experiments are performed in the 1550 nm wavelength regime using silicon waveguides but could be easily extrapolated to other wavelengths and materials. It deserves to be mentioned that 2D grating couplers have been used in silicon photonics as efficient polarization splitters [14–17], but their underlying physical phenomenon is completely different: the output light for different incoming polarizations exit at 90° to each other, and opposite outputs are excited by the same polarization due to symmetry. Here, we achieve the sorting of polarizations into parallel and opposite directions based entirely on polarization asymmetry and mirror-symmetry breaking in the orthogonal direction.

Figure 1 shows the basic idea. Linearly polarized light impinges on a scatterer (we designed a rectangular structure with sides $w_x = 300$ nm and $w_y = 400$ nm) fabricated on a silicon waveguide of standard dimensions (220 nm × 400 nm). The structure scatters light which, in the near field, couples to the fundamental transverse electric (TE) mode of the silicon waveguide. For a linear polarization at an angle, θ, with the y axis, the near field vectorial interference of such scattering results in the excitation of the waveguide modes only in one direction. While the explanation in terms of near field interference is intuitive when considering a single dipole scatterer [8] and inspired us in this design, here, the scattering is not simple, so a simpler very general explanation can be given instead, using the superposition principle, by studying the scattering of the horizontally and vertically polarized components of the incident light into the waveguide modes, as described below.

General symmetry considerations imply that, for any horizontally mirror-symmetric scatterer, an incident

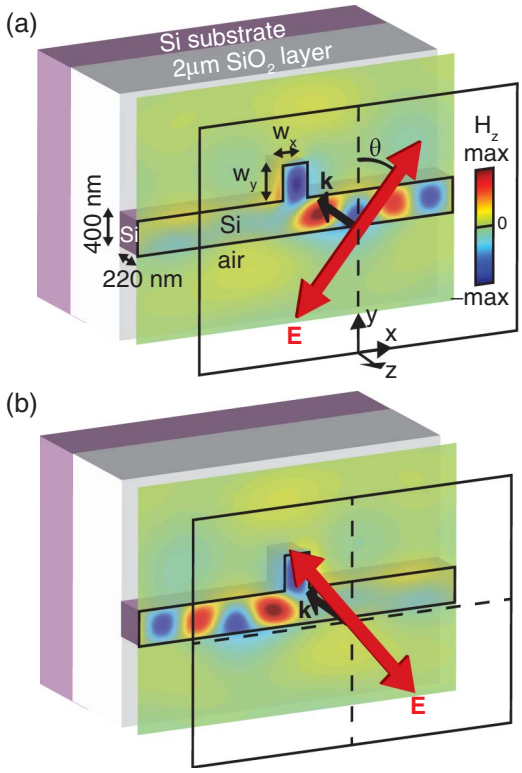

Fig. 1. Sorting of polarized photons in a silicon waveguide with a single scatterer: numerical simulation showing the instantaneous magnetic field z component at the middle plane of the waveguide for a normally incident, monochromatic $\lambda = 1583$ nm plane wave linearly polarized at (a) $\theta = 30°$ and (b) $\theta = -30°$.

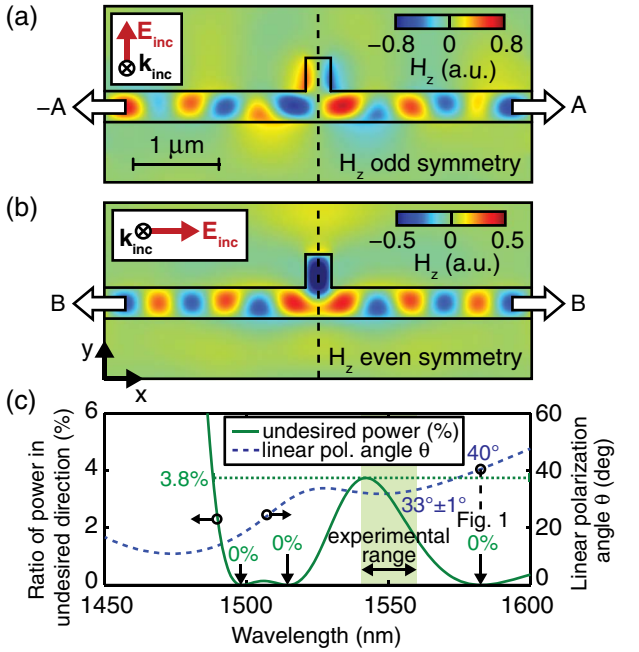

Fig. 2. Symmetry explanation of the phenomenon: (a) and (b) numerical simulation showing the instantaneous H_z at the middle plane of the waveguide for a normally incident monochromatic $\lambda = 1583$ nm plane wave with (a) vertical polarization, $\theta = 0°$ and (b) horizontal polarization, $\theta = 90°$. (c) Ratio of power between the undesired and the desired direction $R = (A - (\beta/\alpha)B)/(A + (\beta/\alpha)B)$. If we limit ourselves to linear polarizations $(\beta/\alpha) \in \Re$, the optimal contrast R is obtained when $(\beta/\alpha) = |A/B|\cos(\arg(A/B))$. The associated linear polarization angle $\theta = \tan^{-1}(\beta/\alpha)$ is plotted.

vertical polarization $\mathbf{E_{inc}} = E_0 \exp(ikz)\hat{\mathbf{y}}$ excites the guided TE mode with complex amplitudes $+A$ to the right $(+x)$ and $-A$ to the left $(-x)$ [see Fig. 2(a)], while a horizontal polarization $\mathbf{E_{inc}} = E_0 \exp(ikz)\hat{\mathbf{x}}$ excites both directions of the TE guided modes with the same complex amplitude, B [see Fig. 2(b)]. Applying the superposition principle, the interference between fields with an even and odd x symmetry results in the unidirectionality shown in Fig. 1.

Mathematically, any normally incident plane wave can be written as $\mathbf{E_{inc}} = E_0 \exp(ikz)(\alpha\hat{\mathbf{y}} + \beta\hat{\mathbf{x}})$, where α and β are complex coefficients determining the polarization. Applying the superposition principle, this general situation corresponds to a simple weighted addition of the fields in Figs. 2(a) and 2(b) so that the waveguide TE mode will be excited with amplitudes $\beta B + \alpha A$ to the right side and $\beta B - \alpha A$ to the left. A perfect unidirectionality with ratio 1:0 can be achieved under the simple condition $\beta = (A/B)\alpha$, where all quantities are complex, and it requires, in general, an elliptical polarization. A and B can be easily obtained from numerical simulations and show a dispersive behavior, and optimization algorithms are easily applied to the scatterer design. Changing $\beta \to -\beta$ switches to the opposite propagation direction, as shown in Fig. 1(b). Mirroring vertically the whole structure (including scatterer and waveguide) is mathematically equivalent to changing $\alpha \to -\alpha$, and also switches the propagation direction; thus, the relative placement of the scatterer and the waveguide is an essential ingredient of the observed directionality. From all the above we can deduce two general fundamental requirements to achieve asymmetrical excitation in the mirror-symmetric x axis: (i) the incoming polarization must not be fully parallel nor perpendicular to the mirror-symmetry plane $(\alpha, \beta \neq 0)$, and (ii) the whole structure must have a broken mirror symmetry in the y axis (otherwise $B = 0$; i.e., the incoming H polarization does not excite the TE waveguide mode for a y-symmetric structure). Both are general requirements imposed by symmetry arguments. We include a y-mirror-symmetric structure in our experiments (see Fig. 3) as a control scatterer that shows a completely symmetric power splitting with no unidirectionality. In other works, grazing incidence is used to achieve the fundamental requirement of breaking the y-mirror symmetry [8,11].

In our design, our aim was to achieve unidirectionality when the incident polarization is linear; i.e., α and β have equal phase. Under this condition, ideal unidirectionality requires that the phases of A and B are equal. At the wavelengths where this happens, a linear polarization will achieve theoretically a perfect 1:0 contrast. In our design, A and B have a very similar phase (<22° difference) throughout the entire range of telecommunication wavelengths, meaning that the ideal 1:0 contrast condition would require a very eccentric, close to linear, incoming polarization ellipse. In practice, as shown by the simulations and experiments, an incoming linear polarization is sufficient for high contrast ratios in that range. Figure 2(c) plots the ratio of power, R, between

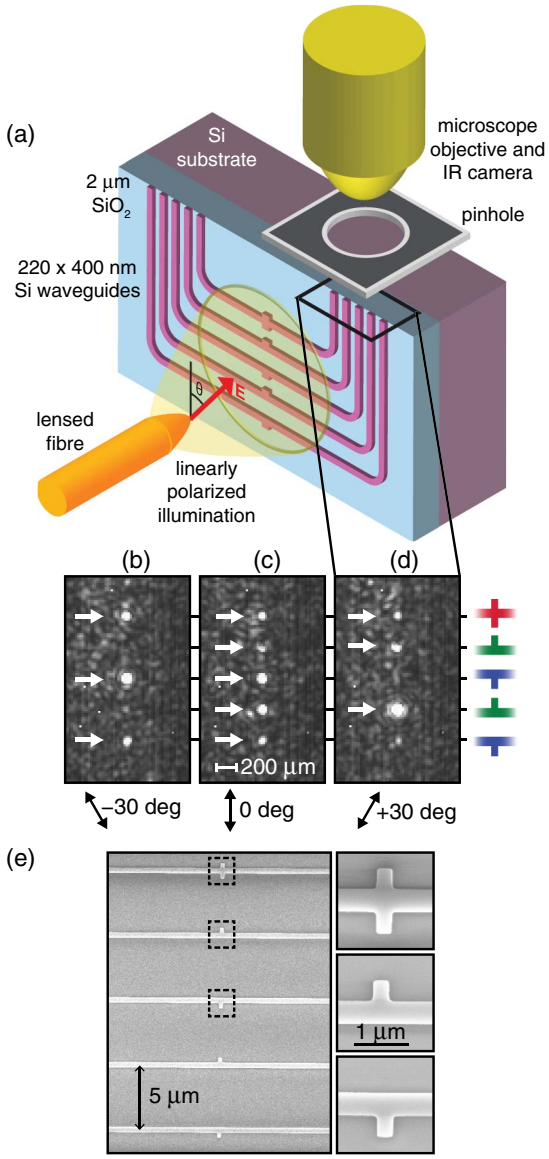

Fig. 3. Experimental setup: (a) depiction of the experimental setup (not to scale); (b)–(d) infrared images of the waveguide output spots captured by the camera for three different linear polarization illuminations of the lensed fiber ($\lambda = 1550$ nm); (e) scanning electron micrograph (SEM) image of the scatterers in the fabricated and measured sample.

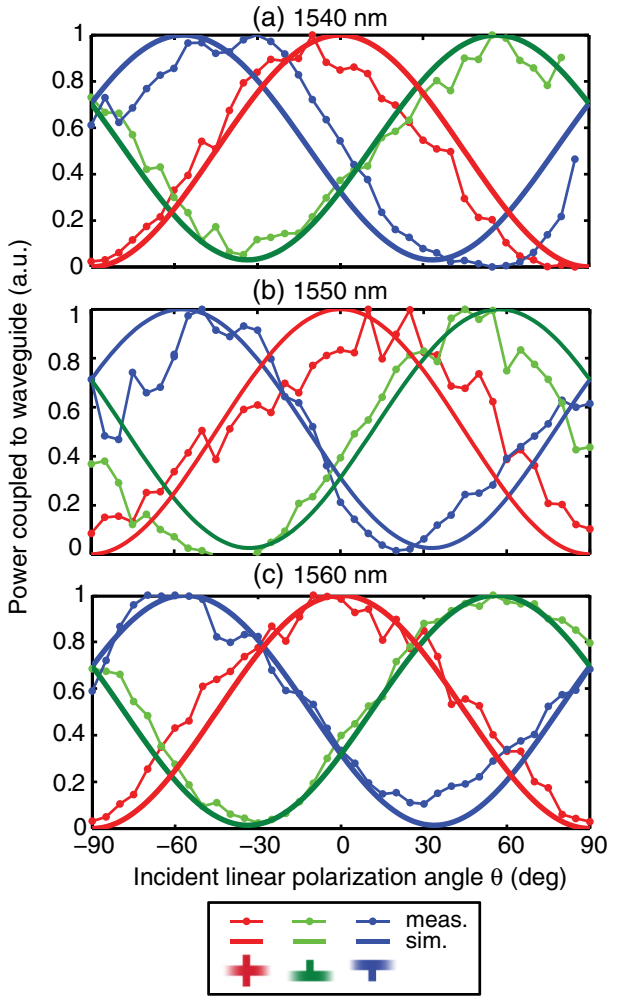

Fig. 4. Broadband measurements: measured and simulated output power of the waveguides for different angles of incident linear polarization at (a) 1540 nm, (b) 1550 nm, and (c) 1560 nm, obtained by processing the infrared images from the camera at different wavelengths.

the undesired and the desired direction when using the optimal linear polarization. The points where $R = 0\%$ correspond to frequencies in which the phases of A and B are equal. The angle, θ, of the linear polarization required to maximize the contrast is also plotted in Fig. 2(c) and depends directly on A and B. In our case, at a wavelength of 1583 nm we theoretically achieve ideal 1:0 unidirectionality at $\pm 40°$ (plotted in Fig. 1). In the wide region around telecommunication C-band wavelengths that we measured, 1540–1560 nm, we theoretically predict a unidirectionality ratio always better than 25:1 and a very stable polarization angle $\theta \approx 33°$ of photon sorting, with variations smaller than 1° in the entire range.

Our designed scatterer can also be regarded as a receiving antenna with an effective area (defined as the ratio between the power excited in the waveguide and the incident power density) of ~3200 nm^2 (at 1560 nm), which is 27% of its physical area. This allows a very simple experimental realization. No attempt at improving this efficiency was done for this proof of principle experiment, but improving the nanoantenna design while maintaining the same principle is a straightforward engineering task.

A depiction of our experimental setup is shown in Fig. 3(a). A lensed fiber is used to illuminate five different scatterers with linearly polarized light. The polarization is controlled with a fiber polarization controller, and monitored with a free space linear polarizer and IR camera placed behind the substrate (not shown). One of the scatterers is our control scatterer, mirror-symmetric in the y direction. The others are two pairs of the designed scatterers with the same dimensions but mirrored in y, thus exhibiting opposite directionality. The light excited into each waveguide is guided toward the edge of the sample, where the waveguides are cut and radiate light through a pinhole (to avoid collecting noise light from the nearby lensed fiber) into a microscope objective with an IR

camera that can image the intensity of the 5 different outputs. Figures 3(b)–3(d) show the obtained IR images at 1550 nm for three different fiber illumination polarizations, demonstrating clearly the polarization sorting of photons. Figure 3(e) shows a scanning electron micrograph of the fabricated structure. As a quantitative proof, Fig. 4 shows the graphs of the different spot intensities at 1540, 1550, and 1560 nm measured for different input polarization angles, in steps of 5 deg, compared with the expected results obtained from simulations, demonstrating the large bandwidth of the effect.

Based on a single subwavelength-size scatterer, a relatively broad bandwidth and good performance of linear polarization selection is achieved. Clearly, more complex scatterers with a greater parameter space would allow improved designs and different functionalities; for example, sorting of circularly polarized light could be designed by aiming at $A = \pm iB$. For practical applications, a chain or array of periodically spaced scatterers interfering constructively would increase the effective area of the device, at the cost of a resonant behavior. Our demonstrated structure has applications ranging from polarization (de)multiplexing and directional light coupling to polarization-controlled switching and manipulation of polarization-encoded photons in photonic integrated circuits aimed at quantum computing purposes. Reciprocity implies that this type of scatterer can also act as a transmitting antenna with two input silicon waveguides, with applications as a dielectric nanoantenna with controllable polarization in the radiated light [18].

This work has received financial support from the Spanish government (contracts Consolider EMET CSD2008-00066 and TEC2011-28664-C02-02) and GV (grant ACOMP/2013/013). F. J. R.-F. acknowledges support from grant FPI of GV. D. Puerto acknowledges support from grant Juan de la Cierva (JCI-2010-07479).

References

1. P. J. Winzer, A. H. Gnauck, C. R. Doerr, M. Magarini, and L. L. Buhl, J. Lightwave Technol. **28**, 547 (2010).
2. A. Crespi, R. Ramponi, R. Osellame, L. Sansoni, I. Bongioanni, F. Sciarrino, G. Vallone, and P. Mataloni, Nat. Commun. **2**, 566 (2011).
3. P. Tuchscherer, C. Rewitz, D. V. Voronine, F. J. García de Abajo, W. Pfeiffer, and T. Brixner, Opt. Express **17**, 14235 (2009).
4. M. Sukharev and T. Seideman, Nano Lett. **6**, 715 (2006).
5. M. Stockman, S. Faleev, and D. Bergman, Phys. Rev. Lett. **88**, 067402 (2002).
6. M. Aeschlimann, M. Bauer, D. Bayer, T. Brixner, F. J. García de Abajo, W. Pfeiffer, M. Rohmer, C. Spindler, and F. Steeb, Nature **446**, 301 (2007).
7. M. Aeschlimann, M. Bauer, D. Bayer, T. Brixner, S. Cunovic, A. Fischer, P. Melchior, W. Pfeiffer, M. Rohmer, C. Schneider, C. Strüber, P. Tuchscherer, and D. V. Voronine, New J. Phys. **14**, 033030 (2012).
8. F. J. Rodríguez-Fortuño, G. Marino, P. Ginzburg, D. O'Connor, A. Martínez, G. A. Wurtz, and A. V. Zayats, Science **340**, 328 (2013).
9. J. Lin, J. P. B. Mueller, Q. Wang, G. Yuan, N. Antoniou, X.-C. Yuan, and F. Capasso, Science **340**, 331 (2013).
10. N. Shitrit, I. Yulevich, E. Maguid, D. Ozeri, D. Veksler, V. Kleiner, and E. Hasman, Science **340**, 724 (2013).
11. S.-Y. Lee, I.-M. Lee, J. Park, S. Oh, W. Lee, K.-Y. Kim, and B. Lee, Phys. Rev. Lett. **108**, 213907 (2012).
12. L. Huang, X. Chen, B. Bai, Q. Tan, G. Jin, T. Zentgraf, and S. Zhang, Light Sci. Appl. **2**, e70 (2013).
13. B. B. Tsema, Y. B. Tsema, M. R. Shcherbakov, Y.-H. Lin, D.-R. Liu, V. V. Klimov, A. A. Fedyanin, and D. P. Tsai, Opt. Express **20**, 10538 (2012).
14. X. S. Yao, L.-S. Yan, B. Zhang, A. E. Willner, and J. Jiang, Opt. Express **15**, 7407 (2007).
15. D. Taillaert, P. I. Borel, L. H. Frandsen, R. M. De La Rue, and R. Baets, IEEE Photon. Technol. Lett. **15**, 1249 (2003).
16. D. Taillaert, W. Bogaerts, P. Bienstman, T. F. Krauss, P. Van Daele, I. Moerman, S. Verstuyft, K. De Mesel, and R. Baets, IEEE J. Quantum Electron. **38**, 949 (2002).
17. W. Bogaerts, D. Taillaert, P. Dumon, D. Van Thourhout, R. Baets, and E. Pluk, Opt. Express **15**, 1567 (2007).
18. F. J. Rodríguez-Fortuño, D. Puerto, A. Griol, L. Bellieres, J. Martí, and A. Martínez, "Universal method for the synthesis of arbitrary polarization states radiated by a nanoantenna," Laser Photon. Rev. (submitted).